Supplementary information for:

Condenson-related thermoelectric properties and formation of coherent nanoinclusions in Te-substituted In_4Se_3

Mahn Jeong,[a,b] Young Soo Lim,*[a] Won-Seon Seo,[a] Jong-Heun Lee,[b] Cheol-Hee Park,[c] Malgorzata Sznajder,[d] Lyubov Yu. Kharkhalis,[e] Dariya M. Bercha,[e] and Jihui Yang [f]

[a] Energy and Environmental Division, Korea Institute of Ceramic Engineering and Technology, Seoul, Korea, [b] Department of Materials Science and Engineering, Korea University, Seoul, Korea, [c] Corporate R&D, LG Chem/Research Park, Daejeon, Korea, [d] Institute of Physics, University of Rzeszow, Rzeszow, Poland, [e] Institute of Physics and Chemistry of Solid State, Uzhgorod National University, Uzhgorod, Ukraine, [f] Department of Materials Science and Engineering, University of Washington, Seattle, USA.

Corresponding author E-mail: yslim@kicet.re.kr (Y.S. Lim)

Table S1. EDS point analysis results at five arbitrary points from the matrix and from the nanoinclusions in $In_4(Se_{0.95}Te_{0.05})_{2.6}$ compound.

Point analysis	Matrix			Nanoinclusion		
	In (wt%)	Se (wt%)	Te (wt%)	In (wt%)	Se (wt%)	Te (wt%)
#1	69.84	28.52	1.64	85.11	14.35	0.54
#2	71.42	26.83	1.75	77.05	22.42	0.54
#3	68.68	29.25	2.07	75.79	24.39	-0.18
#4	69.41	29.36	1.23	78.65	23.60	-2.24
#5	69.97	28.48	1.54	80.39	19.43	0.18
Average	69.90	28.50	1.60	79.40	20.80	-0.20

Table S2. EDS point analysis results at five arbitrary points from the matrix and from the nanoinclusions in $In_4Se_{2.6}$ compound.

Point analysis	Matrix		Nanoinclusion	
	In (wt%)	Se (wt%)	In (wt%)	Se (wt%)
#1	69.29	30.71	71.50	23.50
#2	70.99	29.01	83.16	16.84
#3	66.28	33.72	72.29	27.71
#4	70.25	29.75	75.01	24.99
#5	72.31	27.69	81.69	18.31
Average	69.80	30.20	76.70	23.30

Figure S1. A HRTEM micrograph of cation-substituted $(In_{0.98}Sn_{0.02})_4Se_{2.6}$ compound along <001> zone axis.

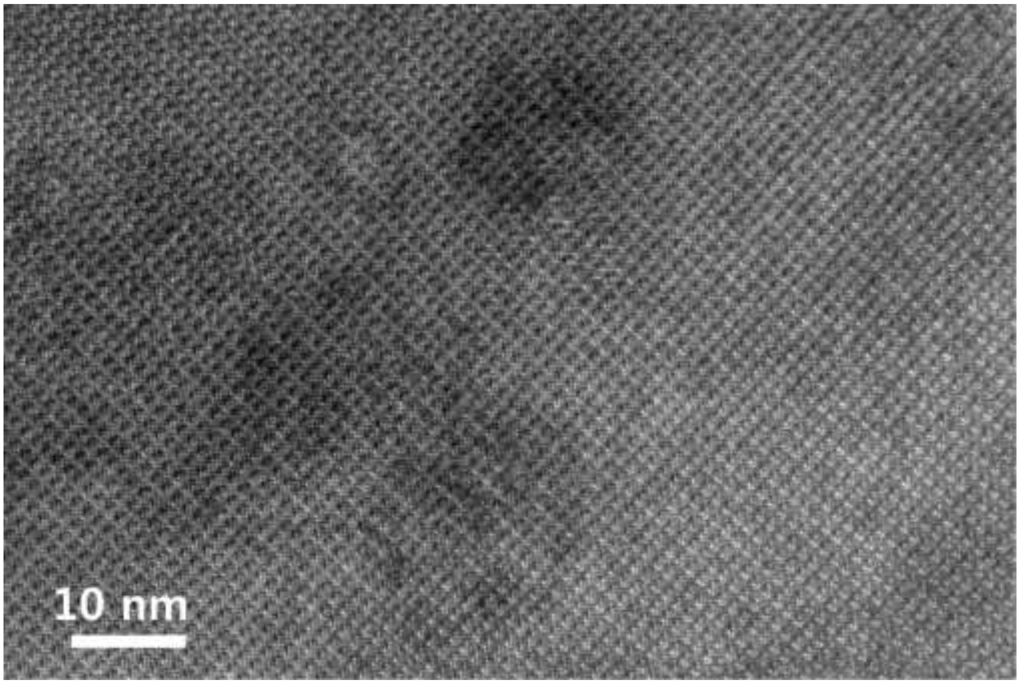

Figure S2. XRD patterns of unalloyed $In_4Se_{2.6}$ and Te-substituted $In_4Se_{3-\delta}$ (IST) compounds. Although a tiny amount of metallic indium was detected, all samples were mostly composed of In_4Se_3 phase. However, no extra XRD peak originating from the nanoinclusion could be observed in the XRD patterns.

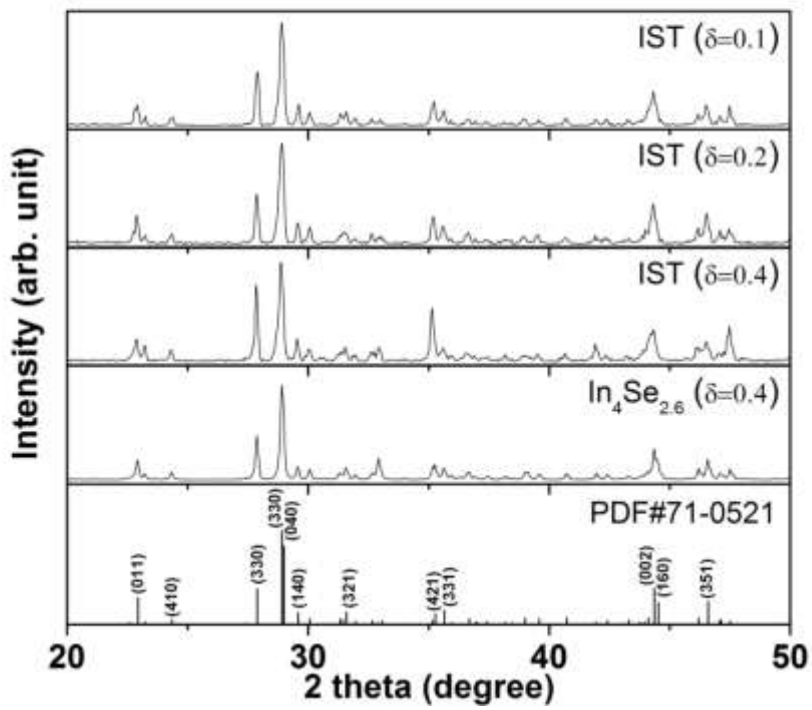

Figure S3. A SEM micrograph of a fractured surface of unalloyed $In_4Se_{2.6}$ compound.

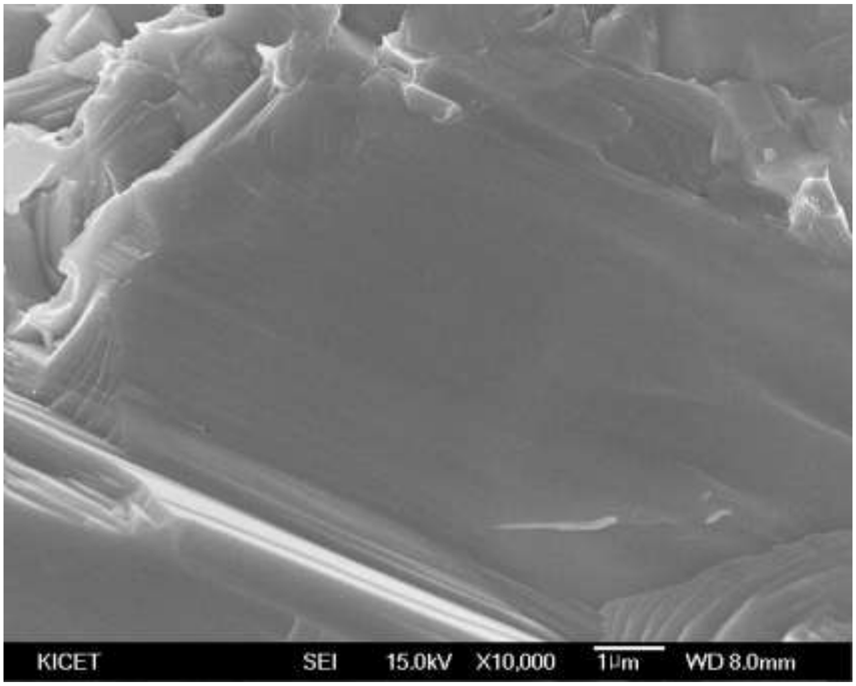

Figure S4. (a) A low-magnification bright-field TEM micrograph of unalloyed $In_4Se_{2.6}$. (b) and (c) are enlarged bright-field TEM micrographs of Grain A and B, respectively. In these figures, the wide distribution of the nanoinclusions can be clearly observed.